Astron. Astrophys. 265, 487–498 (1992)

ASTRONOMY AND ASTROPHYSICS

Molecular-line emission from the centres of Centaurus A and other southern galaxies

F.P. Israel

Sterrewacht, Postbus 9513, 2300 RA Leiden, The Netherlands

Received December 19, 1991; accepted March 3, 1992

Abstract. A variety of molecular lines was observed in emission towards the centre of Centaurus A (NGC 5128). This emission consists of two components. A relatively narrow component is due to the extended molecular disk corresponding to the dust lane crossing the optical image of Cen A. A much broader component corresponds to the circumnuclear disk which has a diameter of about 30″ (750 pc). This disk appears to be warm ($T > 20$ K) and clumpy.

Transitions tracing high-density molecular lines, notably the $J = 1$–0 transitions of HCO^+, HCN and HNC were observed towards the centres of NGC 253, NGC 3256, the Circinus galaxy, and M 83. Except for the distant NGC 3256, all these galaxies exhibit a central molecular line enhancement consistent with the presence of a molecular circumnuclear torus or bar. The main result is the nearly constant ratio of observed molecular line brightness temperatures from galaxy to galaxy. In particular the HCN/HNC ratio shows very little deviation from the mean value of 2.1, indicating warm molecular gas in all galaxies observed, and suggesting a clumpy distribution.

The ratios of HCO^+ and HCN with respect to ^{12}CO and ^{13}CO likewise show little variation, as does the HCN/HCO^+ ratio. With respect to ^{12}CO, both molecules are relatively strong in the circumnuclear disk of Centaurus A. With respect to ^{13}CO, the two molecules are relatively weak in M 83. The $J = 1$–0 ^{13}CO strength in NGC 3256 is unusually low with respect to that of all other molecules observed including ^{12}CO. In all galaxies, the ratio of central HCN/HCO^+ emission to total far-infrared emission is remarkably constant. In contrast, the ratio of central ^{12}CO to total far-infrared emission is a factor of almost three higher in NGC 3256, Circinus and NGC 4945 than in NGC 253, Centaurus A and M 83. The physical meaning of this result is still unclear.

Key words: galaxies: individual (NGC 253, NGC 3256, NGC 4945, M 83, Circinus, Centaurus A) – galaxies: nuclei – molecules – interstellar medium

1. Introduction

Since the IRAS survey, many galaxies are known to be powerful emitters of infrared emission. Modern millimetre telescopes, such as the SEST, allow us to measure molecular line emission from such galaxies. We have selected a sample of relatively nearby galaxies with detected 12 μm emission from the IRAS point source catalog on the assumption that unresolved mid-infrared emission from resolved galaxies is a good indicator for the presence of dense molecular material in the central regions of these galaxies. At the same time, we have started a detailed study of molecular line absorption against the nucleus of the nearest radio galaxy, Centaurus A (NGC 5128) which is also a powerful mid-infrared emitter. In this paper, I present results of the measurements of ^{12}CO, ^{13}CO and other molecules towards the centres of Centaurus A and the galaxies with strongest CO emission detected in the survey. As shown in the recent review by Henkel et al. 1991, such measurements have the potential to supply valuable insight into the structure and physical conditions of central molecular gas concentrations in (mildly active) galactic nuclei.

2. Observational procedures

2.1. Observations

All observations in this paper were made with the 15 m SEST telescope at La Silla between May 1988 and January 1991. The emission line measurements of Centaurus A were obtained as a by-product of a detailed study of narrow molecular absorption lines seen towards its nucleus (Israel et al. 1990, 1991) and therefore generally have very long integration times. The other galaxies observed represent the strongest detections in a CO survey of southern hemisphere galaxies with relatively strong 12 micron IR emission. They were observed with significantly shorter integration times than Centaurus A. For these galaxies, only transitions in the 3 mm window were observed with the SEST Schottky receiver. Depending on weather and frequency observed, total system temperatures including the sky were of order 500 K. The data presented here were obtained with a wideband (500 MHz) acousto-optical spectrometer with 720 channels. All measurements were made in dual beam-switching mode (switching frequency 6 Hz) and a throw of about 12′. The pointing accuracy varied over the runs, but was always better than 10″ and frequently better than 6″. For Cen A, the pointing was considerably better as the unresolved nuclear continuum source provided a running check on pointing quality. The pointing on Cen A was thus continuously updated. In particular at frequencies around 230 GHz, individual poorly pointed integrations identified by relatively low continuum levels were discarded. Tables 1a and 1b summarize the observations and integration times. Also given are effective HPW beamsize and the

Table 1a. Observations log Centaurus A

Galaxy	Line	Frequency (GHz)	Date	Beamsize (arcsec)	η_{mb}	t_{int}[a] (min)
Cen A (NGC 5128)	^{12}CO $J=1-0$	115.271	1990/1991	41	0.69	228
	^{13}CO $J=1-0$	110.201	1989	43	0.71	300
	$C^{18}O$ $J=1-0$	109.782	7/90	43	0.71	24
	^{12}CO $J=2-1$	230.538	1990/1991	23	0.51	284
	^{13}CO $J=2-1$	220.399	5/91	23	0.51	60
	HCO^+ $J=1-0$	89.189	1989–1991	56	0.75	900
	$H^{13}CO^+$ $J=1-0$	86.754	7/90	57	0.75	120
	HCN $J=1-0$	88.632[b]	1/91	56	0.75	180
	HNC $J=1-0$	90.663[b]	1/91	55	0.75	288
	HNCO $4_{04}-3_{03}$	87.925	1/91	56	0.75	140
	HC_3N $J=10-9$	90.979	7/90	55	0.75	96
	HC_3N $J=12-11$	109.174	5/91	43	0.71	120
	CN $J=2-1$	226.875[b]	1/91; 5/91	22	0.51	384
	C_3H_2 $3_{22}-3_{13}$	84.728	7/90	57	0.76	154
	CH_3OH 2–1	96.745[b]	7/90	51	0.73	164
	C_4H $N=12-11$	114.202[b]	1/91	41	0.69	40
	H_2CO	218.222	7/90	23	0.51	466
	SiO $J=1-0$, $v=0$	86.847	1/91	57	0.75	272
	SO_2 $3_{13}-2_{02}$	104.029	1/91	45	0.72	156

[a] Total integration time, half of which is on-source.
[b] Multiple lines; central frequency observed.

Table 1b. Observations log other galaxies

Galaxy	Line	Frequency (GHz)	Date	Beamsize (arcsec)	η_{mb}	t_{int}[a] (min)
NGC 253	^{12}CO $J=1-0$	115.271	1/89	41	0.69	8
	^{13}CO $J=1-0$	110.201	1/89	43	0.71	24
	HCO^+ $J=1-0$	89.189	1/91	56	0.75	48
	HCN $J=1-0$	88.632	1/91	56	0.75	36
	HNC $J=1-0$	90.663	1/91	55	0.75	36
	C_2H $N=1-0$	87.317	1/91	56	0.75	80
	C_3H_2 $2_{12}-1_{01}$	85.339	1/91	57	0.76	166
	C_4H $N=12-11$	114.202	1/91	42	0.70	160
NGC 3256	^{12}CO $J=1-0$	115.271	5/88	41	0.67	20
	^{13}CO $J=1-0$	110.201	1/89	43	0.71	70
	HCO^+ $J=1-0$	89.189	1/91	56	0.75	100
	HCN $J=1-0$	88.632	1/91	56	0.75	98
Circinus	^{12}CO $J=1-0$	115.271	5/88	41	0.67	24
	^{13}CO $J=1-0$	110.201	5/88	43	0.68	16
	HCO^+ $J=1-0$	89.189	1/91	56	0.75	60
	HCN $J=1-0$	88.632	1/91	56	0.75	48
	HNC $J=1-0$	90.663	1/91	55	0.75	160
NGC 4945	^{12}CO $J=1-0$	115.271	5/88	41	0.67	16
	^{13}CO $J=1-0$	110.201	5/88	43	0.68	48
M 83	^{12}CO $J=1-0$	115.271	1/89	41	0.69	8
	^{13}CO $J=1-0$	110.201	1/89	43	0.71	48
	HCO^+ $J=1-0$	89.189	1/91	56	0.75	60
	HCN $J=1-0$	88.632	1/91	56	0.75	36
	HNC $J=1-0$	90.663	1/91	55	0.75	110

[a] Total integration time, half of which is on-source.

main-beam brightness efficiency used to convert antenna temperatures into main-beam brightness temperatures for the relevant observing run (L.E.B. Johansson, private communication). Because of telescope surface modifications, both have changed over the total period.

2.2. *Data handling*

Resulting spectra are shown in Figs. 1–7. Note that the intensity scale shown is antenna temperature. The spectra have been smoothed by varying degrees in order to optimize signal-to-noise ratios. In all spectra, linear baselines were subtracted, although generally baseline offsets were very small. The subtraction procedure has resulted in the disappearance of the significant continuum associated with the nucleus of Centaurus A.

The central CO profiles of the edge-on galaxy Centaurus A are unusual as they consist of four different components: a continuum, a relatively narrow emission component superposed on a much wider emission component interpreted as a circumnuclear disk (Israel et al. 1991) and blends of very narrow absorption lines. Since the two emission components are most clearly distinguished in the high signal-to-noise $J=2$–1 ^{12}CO profile, we used this as a guide to separate them in the $J=1$–0 ^{13}CO and ^{12}CO profiles, as well as the $J=3$–2 ^{12}CO profile obtained with 20″ CSO beam and published by Israel et al. 1991. The procedure was as follows. Because a rotating torus should have a flat-topped (optically thick lines) or double-peaked (optically thin lines) profile, we approximated the wide emission line component by two Gaussians and tested various fits. The range of permissible fit parameters turns out to be fairly restricted. After subtracting the best fit, we then fitted a single Gaussian to the narrow ^{12}CO component, with the additional constraint that the fitted emission cannot imply more than saturated absorption for the main absorption line component. This assumption likewise allows only a limited range of fit solutions. Figure 1 illustrates the fits used for the $J=2$–1 ^{12}CO profile. The $J=1$–0 ^{13}CO profile was fitted by limiting the maximum velocity width to that of the $J=1$–0 ^{12}CO profile, and by requiring that the ratio of the redshifted absorption lines to the main absorption line does not exceed that of the ^{12}CO lines.

The much weaker HCO^+, HCN and HNC emission resulted in profiles with considerably lower signal-to-noise ratios. More importantly, the absorption features cover the full velocity range of 450 to 650 km s^{-1} of the narrow emission-line component. This is illustrated in Fig. 2 by profiles showing not only the HCO^+ and HCN emission but also the full depth of the absorption. Thus, the profiles of these molecular transitions do allow determination of the parameters of the wide component, but not at all of the narrow component. As the velocity range corresponding to narrow-component emission had no weight in the fit, the results in Table 2a refer exclusively to the circumnuclear disk, as is confirmed by the width of the features found. Moreover, with the observed S/N ratio, there is no meaningful difference between single and double Gaussian fits for these profiles.

In Tables 2a and 2b we give peak main-beam brightness temperatures T_{mb}, central velocities V_{LSR}, half-power velocity widths ΔV and velocity-integrated main-beam brightness intensities I_{mb}. In Table 2b, we have included data on NGC 4945 taken from a paper by Henkel et al. 1990. Our own $J=1$–0 CO data are included to verify the calibration of the two data-

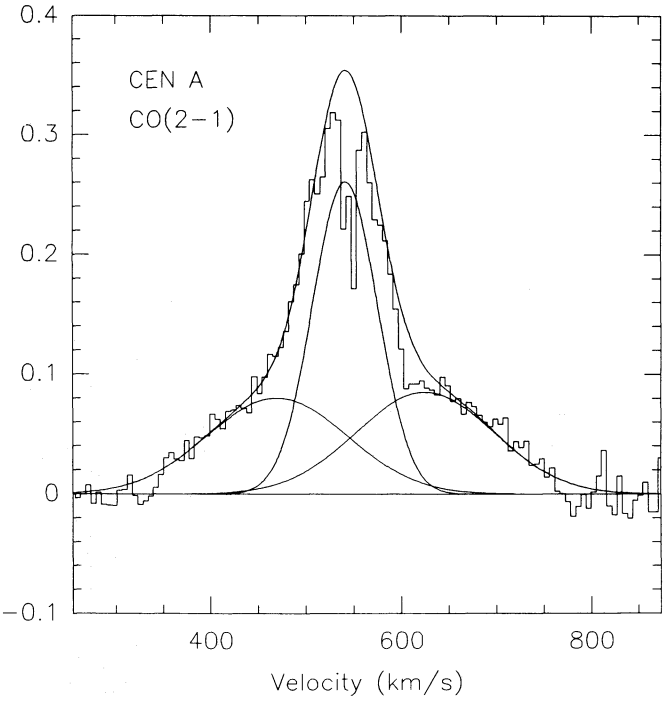

Fig. 1. $J=2$–1 ^{12}CO profile obtained towards the centre of Centaurus A. Smooth solid lines illustrate the fitting procedure used to decompose the profile. Two Gaussians are used to approximate the expected broad, flat-topped profile corresponding to emission from the circumnuclear ring. A single Gaussian, constrained by the observed blue wing and by the maximum intensity permitted by the depth of the main absorption component, is used to approximate the emission from the extended dark band (see Sect. 2.2)

sets. Comparison shows good agreement for the $J=1$–0 CO transitions.

In Table 3 we give the observed integrated line strengths with respect to I_{mb} (^{13}CO). The ^{12}CO lines of NGC 253, NGC 4945 and the Circinus galaxy are flat-topped, whereas the ^{13}CO lines of these galaxies appear to be double-peaked. Such line shapes suggest a molecular distribution characterized by a lack of material in the centre, although it may be possible to envision other interpretations. Deferring possible interpretations of this result to the future, we have decomposed the observed profiles from these galaxies into two ("red" and "blue") Gaussian components. This may not correspond very accurately to the actual physical conditions in these galaxies (for instance, see Whiteoak et al. 1990; Henkel et al. 1991 on NGC 4945), but at least it allows us to compare line ratios for the red and blue profile sides in the same galaxy. Table 4 gives the results of the fitting procedure; it also contains the component central velocities determined from ^{12}CO and ^{13}CO profiles and assumed to be identical for the other molecules.

3. Results and discussion

3.1. *Centaurus A (NGC 5128)*

NGC 5128, site of the strong radio source Centaurus A, appears to be a galaxy merger seen almost edge-on (inclination about 80°; Quillen et al. 1992). The galaxy contains an extremely compact

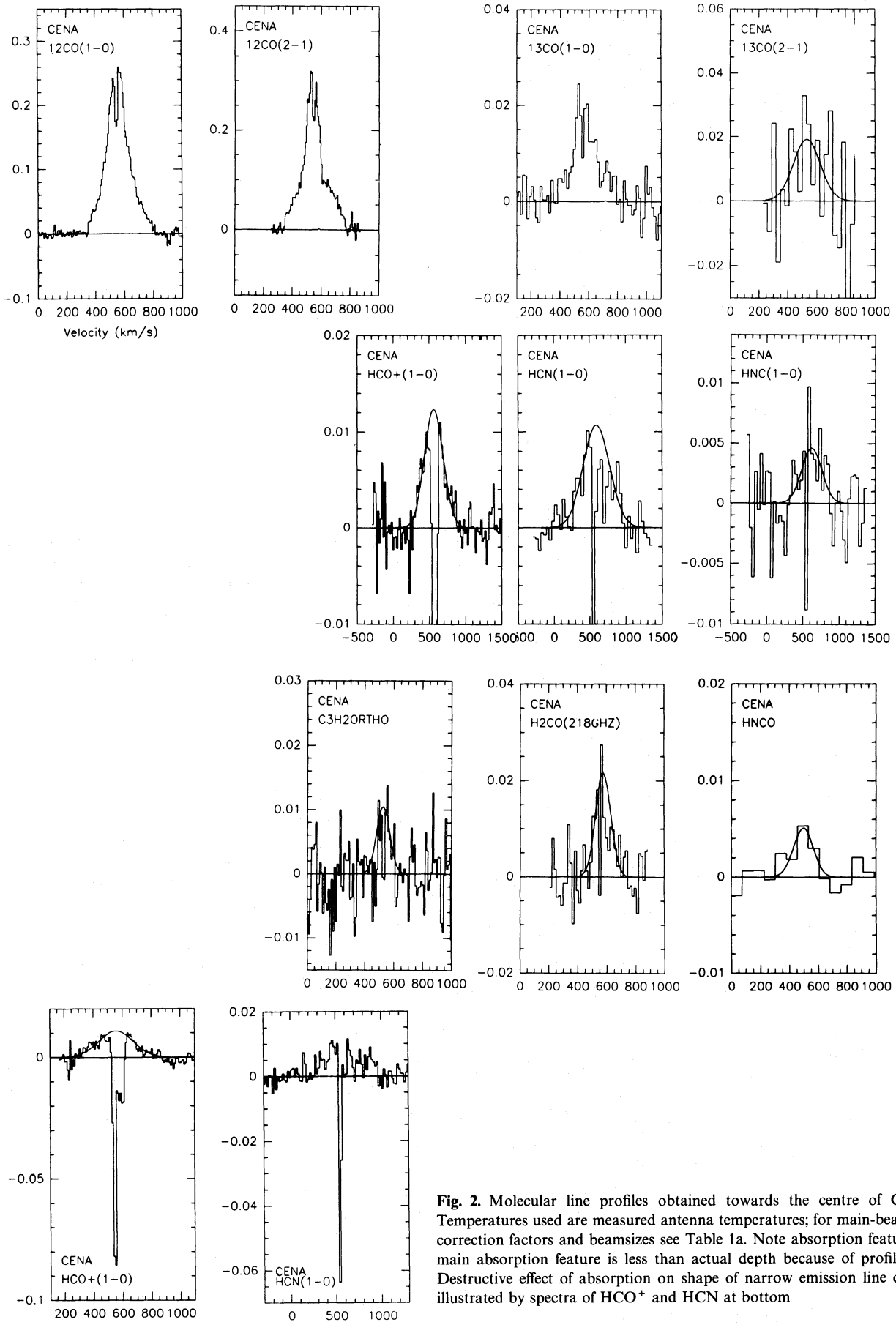

Fig. 2. Molecular line profiles obtained towards the centre of Centaurus A. Temperatures used are measured antenna temperatures; for main-beam brightness correction factors and beamsizes see Table 1a. Note absorption features; depth of main absorption feature is less than actual depth because of profile smoothing. Destructive effect of absorption on shape of narrow emission line component is illustrated by spectra of HCO^+ and HCN at bottom

Table 2a. Fitted[a] line parameters Centaurus A

Component	Transition	T_{mb} (mK)	ΔV (km s^{-1})	V_{LSR} (km s^{-1})	I_{mb} (K km s^{-1})
Narrow	^{12}CO $J=1$–0	380	105	+554	42±6
	^{12}CO $J=2$–1	550	80	+540	46±5
	^{12}CO $J=3$–2[b]	410	80	+543	34±6
	^{13}CO $J=1$–0	35	90	+560	3.1±0.8
Wide	^{12}CO $J=1$–0	90	365	+550	38±4
	^{12}CO $J=2$–1	180	330	+550	65±6
	^{12}CO $J=3$–2	215	300	+550	60 ± 6
	^{13}CO $J=1$–0	11	350	+565	4.1 ± 0.5
	HCO^+	12	360	+553	4.6±0.6
	HCN	12	340	+550	4.4±0.7
	HNC	7	—	—	2.2±0.7
Total	^{13}CO $J=2$–1[c]	37:	—	—	9±2
	HNCO[d]	7	—	—	0.8±0.4
	C_3H_2[d]	13	—	—	1.7±0.4
	H_2CO[d]	43	—	—	5.5±1.5
	$C^{18}O$ $J=1$–0	—	—	—	<1
	$H^{13}CO^+$	—	—	—	<2
	HC_3N $J=10$–9	—	—	—	<1
	HC_3N $J=12$–11	—	—	—	<1
	CH_3OH	—	—	—	<1
	SiO $J=1$–0, $v=0$	—	—	—	<0.3
	CN $J=2$–1	—	—	—	<0.5
	SO_2	—	—	—	<3
	C_4H	—	—	—	<4

[a] See text.
[b] Decomposition of $J=3$–2 ^{12}CO CSO spectrum (Israel et al. 1991).
[c] Fit suggests mostly emission from wide component.
[d] Fit suggests significant contribution by narrow component.

radio (<0.5 10^{-3}″ or <0.01 pc at a distance of 5 Mpc) nucleus which is self-absorbed at frequencies below 10 GHz, but has a strong radio continuum at millimetre wavelengths. Against the nucleus, molecular lines of various species are seen in absorption (in effectively a 0.5 10^{-3}″ pencil beam). In this paper, we will interpret the observed profile as follows. The narrow emission line corresponds to the dark band crossing the optical image of Centaurus A, reaching out to distances of order 3 kpc from the nucleus (cf. Eckart et al. 1990). The wide emission line component corresponds to a distinct circumnuclear disk of maximum radius about 15″, or 400 pc (Israel et al. 1991); note that this disk is only discernible at resolutions of 30″ or better. Its kinematical signature is seen in Fig. 2a of Quillen et al. 1992 as a feature going from (+0.25′, +300 km s^{-1}) to (−0.25′, +700 km s^{-1}). Israel et al. 1990 predicted that far-infrared observations with sufficiently high-resolution, not available at the time, would show the circumnuclear disk directly. Indeed, very recent observations at 450 and 800 μm with 13.5 arcsec resolution resolve a small circumnuclear disk at a position angle about 30° larger than that of the more extended dark band emission (T.G. Hawarden, paper in preparation). The majority of the molecular absorption features seen against the nucleus probably originate in the circumnuclear disk (Israel et al. 1991). Profiles exhibiting both emission and absorption, but not the (subtracted) continuum are shown in Figs. 1 and 2.

As mentioned in Sect. 2.2, the $J=1$–0 ^{12}CO, ^{13}CO and $J=2$–1 ^{12}CO parameters in Table 2a reflect the result of consistent fits; the sum of the velocity-integrated intensities of the fitted components is about 20 per cent higher than the observed intensity integrated over the velocity range of 300–800 km s^{-1}, interpolating the deep central absorption. The difference is easily accounted for by the clearly present but not corrected absorption on the red wing of the narrow emission profile. Note that the ^{12}CO spectra presented here have a signal to noise ratio about a factor of two better than those presented by Israel et al. 1990; in addition, the results presented here differ somewhat from those given by Israel et al. 1990 as a result of the different profile fitting made possible by this higher signal to noise ratio. In the HCO^+, HCN and HNC profiles only the wide component could be fitted. The signal to noise ratio on the $J=2$–1 ^{13}CO, C_3H_2 and HNCO profiles is rather low. However, the narrow width of the latter two line profiles suggests these are mostly due to the dark band. Any possible broad-line emission is not obvious from the profiles in Fig. 2. This is also the case for the H_2CO profile, where a hint of absorption around 600 km s^{-1} is present. Interestingly, observations at 5 GHz by Seaquist & Bell 1990 indicate similar H_2CO

Table 2b. Observed line parameters other galaxies

Galaxy	Transition	T_{mb} (mK)	ΔV (km s^{-1})	V_{LSR} (km s^{-1})	I_{mb} (K km s^{-1})
NGC 253	^{12}CO	1390	230	+250	325±25
	^{13}CO	150	220		28±3
	HCO^+	103	215		24±2.6
	HCN	140	210		30±3.2
	HNC	67	210		14±1.8
	C_2H	33	220		6.1±0.9
	C_3H_2	15	—		2.1±0.5
	C_4H	<10	—		<2
NGC 3256	^{12}CO	385	184	+2776	75±5
	^{12}CO[a]	350	209		77±5
	^{13}CO	14	—		2.0±0.4
	^{13}CO[a]	16	131		2.2±0.4
	HCO^+	15	—		3.1±0.8
	HCN	13	—		3.7±1.4
Circinus	^{12}CO	520	345	+425	185 ± 15
	^{13}CO	43	335		11±1.6
	HCO^+	28	270		7.9±1.0
	HCN	23	240		5.6±0.9
	HNC	11	—		3.1±0.9
NGC 4945	^{12}CO	1685	330	+555	480±35
	^{12}CO[b]	—	—		465
	^{13}CO	93	350		26.5±3
	^{13}CO[b]	—	—		29.6
	$HCO^{+,b}$	79	—		22.2
	HCN[b]	61	—		23.9
	HNC[b]	38	—		11.3
	C_2H[b]	31	—		10.7
M 83 (NGC 5236)	^{12}CO	775	98	+510	81±4
	^{13}CO[c]	70	125		10±1
	HCO^+	41	104		4.7±0.8
	HCN	52	99		5.5±1.3
	HNC	20	—		1.5±0.4

[a] SEST data from Aalto et al. 1991.
[b] SEST data from Henkel et al. 1990.
[c] Velocity scale of ^{13}CO incorrect for M 83 in Fig. 6.

Table 3. Integrated line ratios

Galaxy	^{12}CO/^{13}CO	HCO^+/^{13}CO	HCN/^{13}CO	HNC/^{13}CO	HCN/HNC
NGC 253	11.6±1.5	0.86±0.14	1.07±0.16	0.50±0.08	2.1±0.3
NGC 3256	37±7	1.6±0.5	1.9±0.8	—	—
Circinus	16.8±2.6	0.72±0.14	0.51±0.11	0.28±0.09	1.8±0.6
NGC 4945	18.1±2.2	—	—	—	—
NGC 4945[a]	15.7	0.75	0.81	0.38	2.1
Cen A N	14±4	—	—	—	—
Cen A W	9.3±1.4	1.12±0.19	1.07±0.20	0.54±0.18	2.0±0.7
M 83	8.1±0.9	0.47±0.09	0.55±0.14	0.15±0.05	3.7±1.5
Weighted mean	13.5±5	0.8±0.25	0.85±0.3	0.35±0.10	2.1±0.5

[a] SEST data from Henkel et al. 1990.

Table 4. Line ratios from two-component analysis

Galaxy	Velocity ($km\,s^{-1}$)	$^{12}CO/^{13}CO$	$HCO^+/^{13}CO$	$HCN/^{13}CO$	HCN/HNC
NGC 253	160	9.0±1.6	0.81±0.13	0.77±0.13	1.8±0.7
	290	13.1±1.2	0.89±0.10	1.24±0.13	2.3±0.3
Circinus	340	17.0±3.1	0.7±0.2	0.5±0.2	2.2±1.4
	520	15.2±3.1	0.75±0.2	0.6±0.2	1.7±0.7
NGC 4945	495	27.3±2.9	—	—	—
	670	12.2±1.5	—	—	—
NGC 4945[a]	495	—	1.3	1.4	2.2:
	670	—	0.5	0.4	1.9:

[a] Estimated from SEST data by Henkel et al. 1990; see also text.

absorption against the inner jet some 15 arcsec from the nucleus, but not against the nucleus itself. The reality of our 600 $km\,s^{-1}$ feature is thus uncertain.

For the dark band (narrow component) we find from the observed and beamwidth-corrected ratios I_{2-1}/I_{1-0} and I_{3-2}/I_{2-1} an excitation temperature of at most 15 K, assuming an apparent thickness of 30″ for this extended component (cf. Eckart et al. 1990; Quillen et al. 1992). Because of the strong nuclear absorption, a multi-species analysis of the molecular content of the dark band (extended disk) should be carried out at positions off the nucleus.

The circumnuclear disk has a $J=1$–0 $^{12}CO/^{13}CO$ ratio similar to those of NGC 253 and M 83. However, its $HCO^+/^{13}CO$, $HCN/^{13}CO$ and $HNC/^{13}CO$ ratios, although close to those of NGC 253, are rather different from those of M 83. The HCN/HNC ratio of about 2 suggests kinetic temperatures of about 25 K (cf. Irvine et al. 1987; see NGC 253). The ^{12}CO line ratios likewise indicate a similar temperature, but uncertainties in these ratios only poorly constrain the admissible temperature range. The $J=2$–1 ^{13}CO emission is mostly due to the wide component (circumnuclear disk). Depending on the contribution by the narrow component, the $J=2$–1/$J=1$–0 ^{13}CO ratio may be as high as 2.5. Such a high ratio would also indicate the presence of warm and possibly optically thin molecular gas. We note that in the circumnuclear disk HCO^+ and HCN are stronger than ^{13}CO, which suggests that this disk is dominated by high-density clumps.

3.2. NGC 253

This highly inclined peculiar Sc galaxy is one of the strongest extragalactic IRAS sources. It is also a goldmine for extragalactic molecule observers (cf. Henkel et al. 1991, and references therein). The profiles in Fig. 3 clearly show the presence of the two components listed in Table 4. The SEST beam does not resolve the central source but interferometer observations in CO (Canzian et al. 1988) and in HCO^+ (Carlstrom et al. 1990) show an elongated source with dimensions of 36″ × 12″ (corresponding to a deconvolved linear size of 470 × 130 pc for a distance $D=2.5$ Mpc). Position–velocity maps in HCO^+ (Carlstrom et al. 1990) and the OH 1665 and 1667 MHz absorption lines (Turner 1985) show that most of the molecular material is indeed concentrated in the two velocity components with an angular separation of about 10″. The morphology suggests a circumnuclear torus, although other explanations are possible. The 3 mm continuum source coinciding with the nucleus of NGC 253 is resolved and fills the space between the two molecular peaks (Carlstrom et al. 1990).

The multitransition CO analysis by Wall et al. 1991 shows the presence of hot CO gas ($T_k>100$ K) near the nucleus (see also Mauersberger et al. 1990 and Harris et al. 1991). CO temperatures in the extended source are much lower ($T_k=20$–40 K). Our data show a significant difference in the integrated $^{12}CO/^{13}CO$ ratio of the red and blue components, caused by both a difference in peak intensity ratio and in velocity width. Although the latter may be somewhat uncertain, Fig. 3 clearly shows the former. This is not a pointing artifact, as the signal from NGC 253 was strong enough to allow a five-point "peaking-up" procedure. In both components, the HCO^+ strength relative to ^{13}CO is very similar. However, the blue component has a $HCN/^{13}CO$ ratio that is about two thirds of that of the red component. As we imposed identical central velocities for the two components in all profiles, this may in fact reflect a velocity shift, hence a spatial shift, between HCN on the one hand, and ^{13}CO (and HCO^+) on the other hand (cf. Nguyen-Q-Rieu et al. 1989). Whether or not this is the case, the two velocity components appear to have a different brightness distribution. In view of the relative sizes of the beam (identical for HCN and HCO^+) and the molecular source, this result cannot be due to pointing problems. HCO^+ and HCN have almost identical temperature excitation requirements; the lines are most probably optically thick. Thus, differences in brightness distribution are unlikely to be due to (temperature) excitation or abundance differences. However, as HCN samples preferentially higher spatial densities than HCO^+, the observed variation is most likely due to differences in (clump surface) density (see also Sect. 4).

The HCN/HNC ratio is, within the errors, the same for both components. It is remarkable that the presumably optically thick lines HCN and HNC have very much the same intensity ratio 2.1 ±0.3 as the presumably optically thin lines $H^{13}CN$ and $HN^{13}C$ (2.2±0.5: Mauersberger & Henkel 1991). This indicates that HCN and HNC occur in small dense clumps with a small surface filling factor, so that the number surface density of HCN/HNC clumps is an accurate measure for beam-averaged $H^{13}CN/HN^{13}C$ column density. We thus confirm a similar conclusion reached by Nguyen-Q-Rieu et al. 1989 on different grounds. The

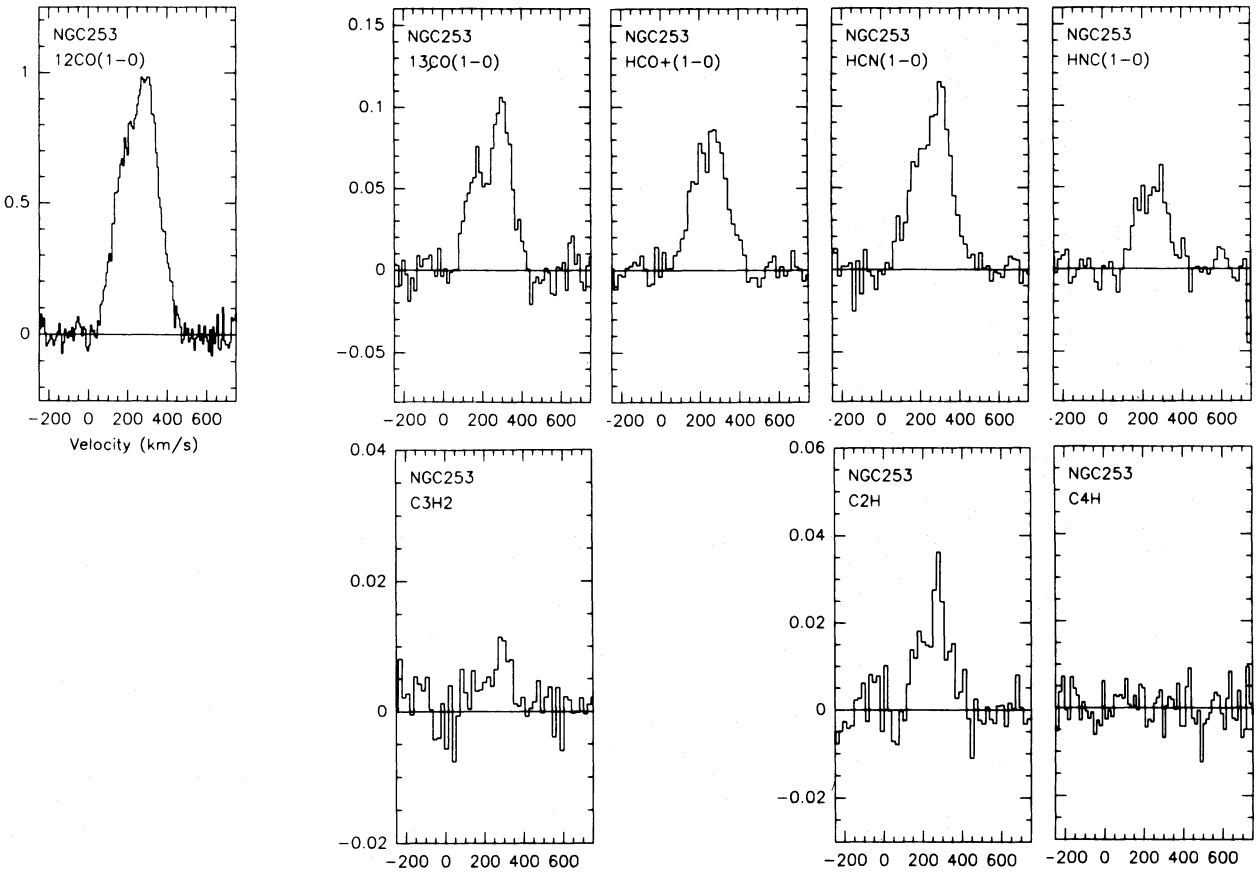

Fig. 3. Molecular line spectra obtained towards the centre of NGC 253. Note non-Gaussian appearance of profiles

diagram by Irvine et al. 1987 suggests that an abundance ratio HCN/HNC = 2 corresponds to a temperature of 20–25 K. The HCN/HCO^+ intensity ratio of 1.25 ± 0.08 in our 55″ beam is very close to the ratio 1.1 found for the inner 20″ of NGC 253 by Nguyen-Q-Rieu et al. 1989.

Whereas C_2H yielded a clear detection, we obtained only an upper limit for C_4H. Taking into account the differences in beamsizes, and assuming a C_2H source size identical to the HCO^+ source size mentioned above, the observed ratio $C_2H/C_4H > 3$ translates into an intrinsic intensity ratio > 5. If this corresponds to an abundance ratio, this ratio is higher than found towards TMC-1, but consistent with the lower limit for the Orion ridge (cf. Irvine et al. 1987; Herbst & Leung 1989).

3.3. NGC 3256

This peculiar galaxy appears to be a pair of merging spiral galaxies (de Vaucouleurs 1956; Toomre 1977). At a distance of 37 Mpc, the SEST beam corresponds to linear sizes of 10 and 7.3 kpc at 88 and 115 GHz respectively. A starburst may be accompanying the merger (e.g. Glass & Moorwood 1985; Rowan-Robinson & Crawford 1989). The galaxy was observed in the $J = 2$–1 ^{12}CO transition (with a 30″ beam) by Sargent et al. 1989 whose data suggest a (deconvolved) FWHM size of 30″ (5.5 kpc) for the molecular material. NGC 3256 has also been observed with SEST in the $J = 1$–0 and $J = 2$–1 transitions of ^{12}CO and ^{13}CO by Aalto et al. 1991, permitting a comparison of our $J = 1$–0 transition results with theirs. The central position used by us coincides within a few arcsec with their revised (0, 0)* position, and yields the same integrated intensity I_{mb} within 3% for ^{12}CO (Fig. 4). Likewise, we find similar values for the integrated ^{13}CO intensity and hence for the $^{12}CO/^{13}CO$ ratio: we find 37 ± 6, whereas Aalto et al. 1991 find 35 ± 5. As a consequence of the low ^{13}CO intensity, not only the $J = 1$–0 $^{12}CO/^{13}CO$ and ^{13}CO $J = 2$–1/$J = 1$–0 ratios are unusually high, but as shown in Table 3 also the $HCO^+/^{13}CO$ and $HCN/^{13}CO$ ratios. In contrast, the $HCO^+/^{12}CO$ and $HCN/^{12}CO$ ratios of NGC 3256 are similar to those of NGC 253, Circinus, NGC 4945 and M 83. Note however, that in all molecular lines, NGC 3256 is very similar to the blue wing of NGC 4945.

Although the profiles of NGC 3256 may represent a blending of different components (see also Aalto et al. 1991) the large fraction of the galaxy disk included in the SEST aperture and the weak signals in all but the ^{12}CO transition prohibit a meaningful analysis of line ratios in a two or more component model.

3.4. Circinus galaxy

This is a low-galactic-latitude ($b = -4°$) large and bright spiral galaxy with an inclination of about 65°. At a distance of about 4 Mpc, it is unusually rich in neutral hydrogen (Freeman et al. 1977) and contains a radio nucleus of size 23×18″ corresponding to 450×350 pc (Whiteoak & Bunton 1985). The nucleus is the site of luminous H_2O masers in the velocity range of 500–600 km s^{-1}

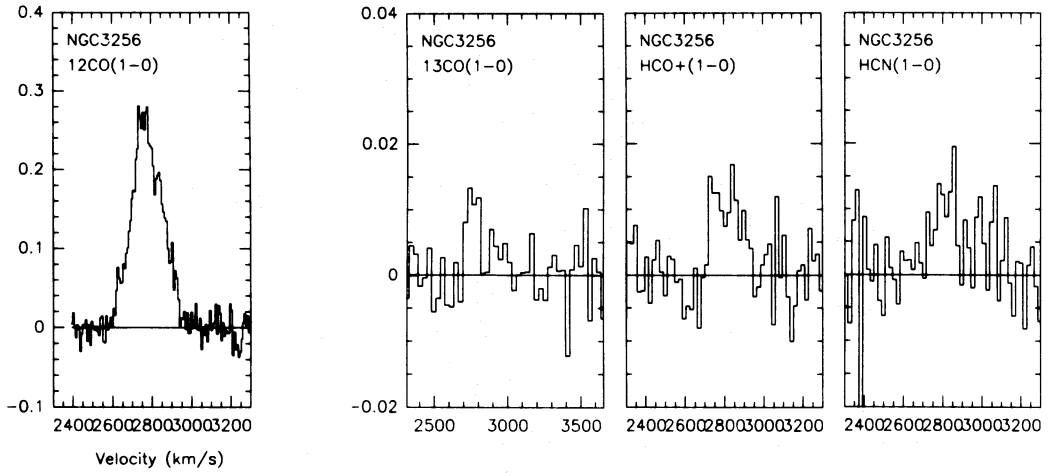

Fig. 4. As Fig. 2, for NGC 3256

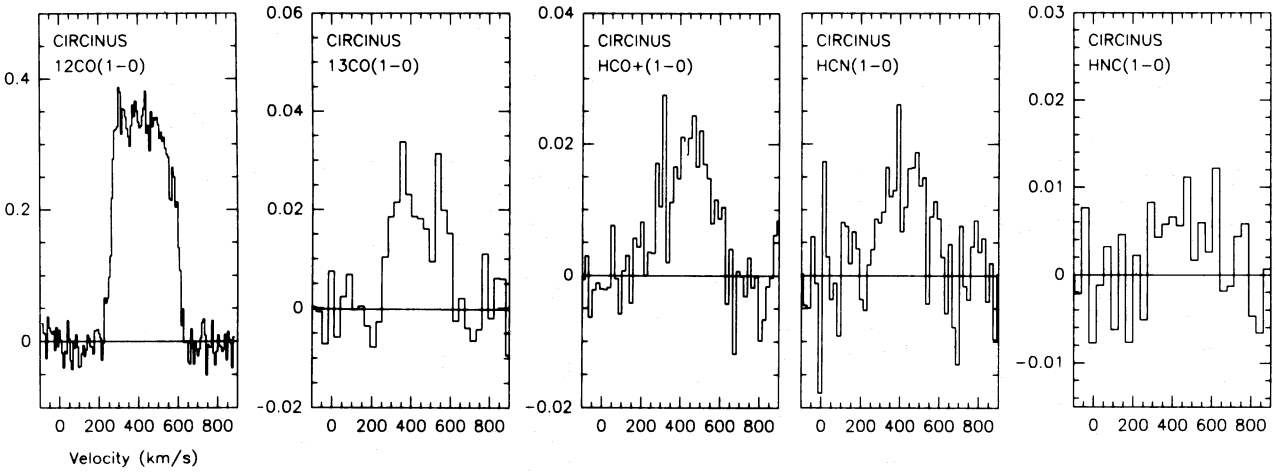

Fig. 5. As Fig. 2, for the Circinus galaxy

(Gardner & Whiteoak 1982; Whiteoak & Gardner 1986). OH absorption ranging from 350–530 km s^{-1} suggests the presence of a rapidly rotating circumnuclear disk (Harnett et al. 1990). The profiles of the Circinus galaxy (flat-topped in ^{12}CO; double-peaked in ^{13}CO) likewise suggest the presence of such a circumnuclear disk or torus (Fig. 5).

The ^{12}CO and HCO$^+$ strengths with respect to ^{13}CO are similar to those in the other galaxies. However, both HCN and HNC are significantly weaker with respect to ^{13}CO and HCO$^+$ (about 60% compared to the other galaxies in Table 3; cf. Nguyen-Q-Rieu et al. 1991). As HCO$^+$ and HCN have very similar excitation requirements, the HCO$^+$/HCN abundance ratio in Circinus may be larger than in the other galaxies; Circinus shares this behaviour with M 82 (Nguyen-Q-Rieu et al. 1989). This situation might be expected for temperatures of order 40–50 K which appears feasible for M 82 (Nguyen-Q-Rieu et al. 1991). However, such temperatures would also lead us to expect an HCN/HNC ratio of order 10 or more, contrary to what is observed (Table 3). Alternatively, some overabundance of HCO$^+$ might result from enhanced shock-ionization (Elitzur 1983). As the luminous H_2O masers in the Circinus nucleus imply significant shock phenomena in the circumnuclear disk (cf. Henkel et al. 1991) this requirement may be met. Finally, the high HCO$^+$/HCN ratio may reflect the relative absence of clumps with the high densities typically sampled by HCN.

As Table 4 shows, the red and blue profile components have line ratios that are identical to within the errors.

3.5. *NGC 4945*

NGC 4945 is a large spiral galaxy at a distance of about 6.7 Mpc. Its nucleus is highly obscured and has radio dimensions of $12 \times 3''$, corresponding to 400×100 pc (Whiteoak & Bunton 1985). It is the site of highly luminous OH and H_2O masers; a good review of the NGC 4945 nucleus was provided by Whiteoak 1986. OH absorption ranging from 350–770 km s^{-1} provides evidence for a circumnuclear disk (Whiteoak & Wilson 1990), as indeed do CO observations that show a rotating disk of (deconvolved) size $33 \times 19''$, corresponding to 1050×600 pc (Fig. 6; Whiteoak et al. 1990). As an extensive survey of nuclear molecular line emission of NGC 4945 was carried out with SEST by Henkel et al. 1990, we observed only the ^{12}CO and ^{13}CO profiles to obtain a means of tying their observations into our sample. The respective ^{12}CO and ^{13}CO integrated intensities I_{mb} agree within

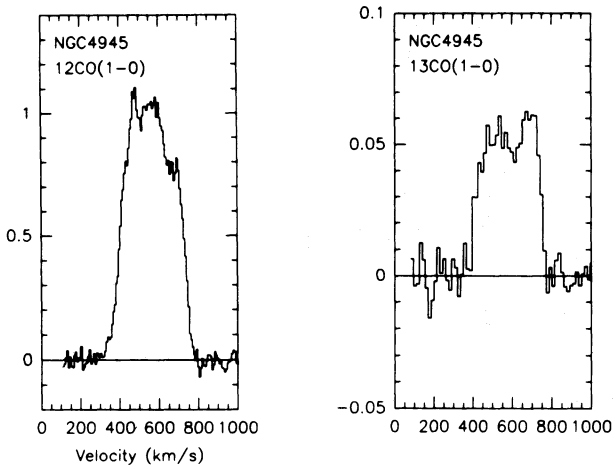

Fig. 6. ^{12}CO and ^{13}CO profiles towards the centre of NGC 4945; see text

5%. As is clear from Table 3, the various line ratios implied by the observations by Henkel et al. 1990 are very similar to those of the other galaxies in our sample.

At high S/N ratios, the ^{12}CO profile of the centre of NGC 4945 shows considerable structure (Whiteoak et al. 1990). Similar structure is seen in the profiles presented by Henkel et al. 1990, notably those of HCO^+ and HCN. They interpret this as indicating the presence of two concentric molecular rings, with additional noncircular motions. However, as an alternative one might consider a single, but inhomogeneous molecular torus. In Table 4 we have used the profiles published by Henkel et al. 1990 to derive line ratios assuming only two velocity components. This may or may not represent a physically meaningful situation, but its main purpose is to show that in NGC 4945 the red and blue components show larger, significant variations in their line ratios than the other galaxies. In particular, the blue wing of NGC 4945 shows line ratios that are similar to the unusual ratios of NGC 3256. For a more detailed discussion we refer to Henkel et al. 1990.

3.6. M 83 (NGC 5236)

M 83 is a bright, nearly face-on (inclination 24°) spiral galaxy at a distance of 3.7 Mpc. It is a well-studied galaxy, and high-resolution CO maps of the centre show an elongated concentration around the nucleus which is usually described as a bar (cf. Handa et al. 1990; Wall 1991; references therein). Both the gaseous disk of M 83 and the central CO condensation of dimensions 40″ × 20″ show a velocity field indicative of significant noncircular motion. The data do not rule out that the central CO condensation is in fact a tilted circumnuclear disk. CO excitation and density were studied by Wall 1991. He concludes that most of the mass resides in cold ($T = 10$ K) low-density molecular gas, but that most of the CO luminosity arises in rather warm (of order 100 K) and dense molecular gas optically thin in ^{12}CO. Indeed, our data (Fig. 7) and Wall's data imply $^{12}CO/^{13}CO$ ratios 8.1 ($J = 1$–0, 43″), 4.6–6.0 ($J = 2$–1, 22″) and 26 respectively > 30 ($J = 3$–2, 22″). High molecular gas temperatures are also consistent with the HCN/HNC brightness temperature ratio 3.7 ± 1.5. In M 83, the strength of HCO^+, HCN and HNC with respect to ^{13}CO is low compared to those of the other galaxies. However, with respect to ^{12}CO these species have strengths similar to those of the other galaxies except Centaurus A.

4. Concluding remarks

Given the complexity of molecular line strengths as a function of excitation temperature, optical depth, volume filling factor and indeed spatial distribution it is difficult to interpret the data presented in this paper in terms of column densities and abundances. Evidence for significant variation in physical conditions on scales smaller than 40–50″, for instance, exists for several of the sample galaxies such as NGC 4945 (blue wing versus red wing; see Fig. 6; Henkel et al. 1990) and M 83 (Wall 1991). It would be surprising if this were not the case for the other galaxies as well, and this makes a straightforward interpretation of measurements averaged over many kpc^2 in a dynamically and radiatively active environment extremely hazardous.

It should also be noted that the line ratios in Table 3 do not take into account the different beamsizes of the SEST in the

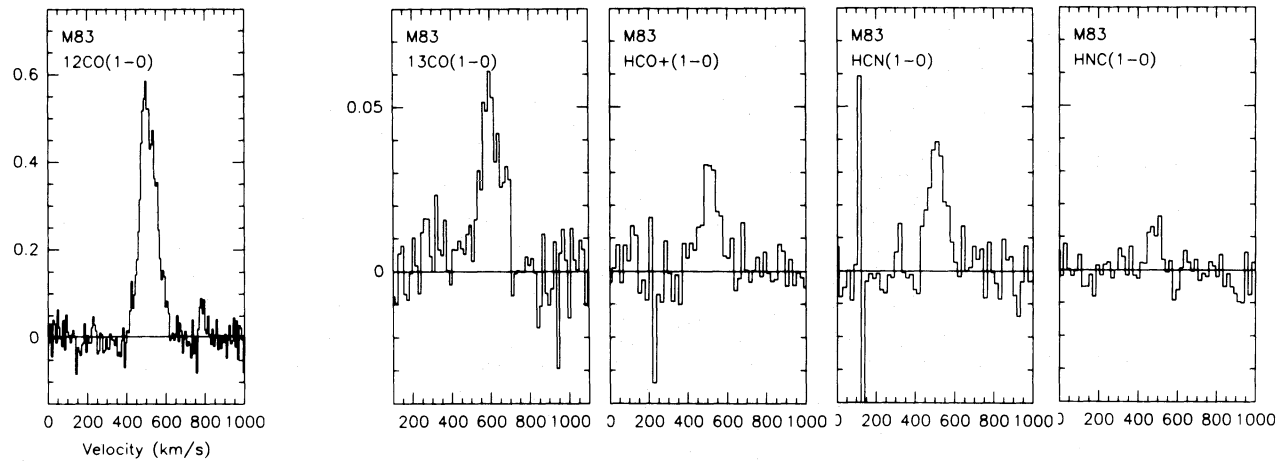

Fig. 7. As Fig. 2, for M 83 (NGC 5236)

85–90 GHz range and the 110–115 GHz range, causing greater beam dilution for HCO^+, HCN and HNC than for ^{12}CO and ^{13}CO in the case of unresolved sources. High resolution CO maps suggest this is the case for all galaxies in the sample; comparison of the HCN and HCO^+ integrated strengths of NGC 253 and M 83 from this paper with those measured by Nguyen-Q-Rieu et al. 1991 in a 25″ beam suggests likewise. The net effect is to raise the ratios in columns 3, 4 and 5 by about a factor of 1.7 if the high-density molecules have the same spatial distribution as ^{13}CO.

The galaxies in this paper all have in common rather strong emission in the mid- and far-infrared as well as in CO from their central regions. Literature data, and the profiles presented in this paper show that most of them contain a circumnuclear disk or torus with diameters of 0.5–1 kpc. However, the nature of these galaxies may be rather different. Nevertheless, the constancy of the observed molecular line brightness temperature ratios is quite remarkable. This is particularly so for the HCN/HNC ratio which indicates mean molecular gas temperatures roughly of order 25 K. The fact that in addition the brightness temperature ratio of the presumably optically thick HCN/HNC in NGC 253 is the same as that of the optically thin $H^{13}CN/HN^{13}C$ suggests a clumpy distribution with a relatively small surface filling factor.

The $HCO^+/^{13}CO$ and $HCN/^{13}CO$ ratios are all within a factor of two of the mean value. In view of the errors this variation, although not large, is significant. The peculiar merger galaxy NGC 3256 has the highest ratio, whereas M 83 has the lowest. If instead we compare HCO^+ and HCN to ^{12}CO, the variation is significantly less. However, now the circumnuclear disk of Centaurus A has $HCO^+/^{12}CO$ and $HCN/^{12}CO$ ratios that are twice as high as those of the other galaxies. The mean (beam-corrected) ratio of $HCO^+/^{12}CO$ and $HCN/^{12}CO$ is about 0.03. This compares very well with the result shown in Fig. 2 of Nguyen-Q-Rieu et al. 1991, after their rather different beamsizes have been taken into account. The HCN/HCO^+ ratio of Circinus of 0.71 ± 0.12 is somewhat low as compared with the mean HCO^+/HCN ratio of 1.2 ± 0.2 of the other galaxies. This result is very similar to that obtained by Nguyen-Q-Rieu et al. 1991 who list this ratio for ten galaxies, including M 83 and NGC 253. In their sample, NGC 3079 and Maffei 2 have significantly higher ratios of >6.8 and 2.6 respectively, while M 82 has a low ratio of 0.5 comparable to that of Circinus. This may indicate that the latter two contain warmer than average molecular gas, suffer from stronger than average (shock) ionization processes, or are depleted in material corresponding to densities of the order of the critical density for HCN.

Finally, we compared the detected molecular line emission to the total far-infrared emission from the same galaxies (taken from IRAS 1989 and Rice et al. 1988). Even though the molecular line strength refers only to the central regions, and the far-infrared strength to all of the galaxy, the HCO^+ and HCN strengths turn out to be closely related to the far-infrared strength. The mean ratio HCO^+/FIR is $5.0 \pm 0.7\ 10^{11}$ (K km s^{-1}/W m^{-2}) and ranges from $2.8\ 10^{11}$ (M 83) to $6.7\ 10^{11}$ (NGC 3256). The mean ratio HCN/FIR is $5.2 \pm 0.8\ 10^{11}$ and ranges from $3.2\ 10^{11}$ to $8.0\ 10^{11}$ for the same galaxies. A comparison of ^{12}CO central strengths to total far-infrared strengths yields a different result: NGC 253, Centaurus A and M 83 are within about 10% from the ratio $^{12}CO/FIR = 5.5\ 10^{12}$ (K km s^{-1}/W m^{-2}), while NGC 3256, Circinus and NGC 4945 are within 10% of $^{12}CO/FIR = 15\ 10^{12}$, or almost three times higher. This confirms the result by Solomon et al. 1992 that HCN correlates much better with far-infrared emission than ^{12}CO, but it raises an intriguing question: what is the physical connection between central molecular cloud complexes and the far-infrared emission of presumably globally distributed dust clouds?

Acknowledgements. It is a pleasure to thank the personnel of the Swedish-ESO Submillimetre Telescope for their invaluable help and advice during the observations. I would also like to thank Th. de Graauw, F. Baas and F. Helmich for obtaining part of the observations presented in this paper. I benefited from discussions with E.F. van Dishoeck, while critical remarks by an anonymous referee led to an improvements in the presentation.

References

Aalto S., Black J.H., Booth R.S., Johansson L.E.B., 1991, A&A 247, 291
Canzian B., Mundy L.G., Scoville N.Z., 1988, ApJ 333, 157
Carlstrom J.E., Jackson J.E., Ho P.T.P., Turner J.L., 1990, in: Hollenbach D.J., Thronson H.A. (eds.) The Interstellar Medium in External Galaxies. Washington D.C.: NASA Conf. Pub. 3084, p. 337
de Vaucouleurs G., 1956, Mem. Mt. Stromlo Observatory III, No. 13
Eckart A., Camerson M., Rothermel H., Wild W., Zinnecker H., Rydbeck G., Olberg M., Wiklind T., 1990, ApJ 363, 451
Elitzur M., 1983, ApJ 267, 174
Freeman K.C., Karlsson B., Lynga G., Burrell J.F., van Woerden H., Goss W.M., 1977, A&A 55, 445
Gardner F.F., Whiteoak J.B., 1982, MNRAS 201, 13P
Glass I.S., Moorwood A.F.M., 1985, MNRAS 214, 429
Handa T., Nakai N., Sofue Y., Hayashi M., Fujimoto M., 1990, PASJ 42, 1
Harnett J.I., Whiteoak J.B., Reynolds J.E., Gardner F.F., Tzioumis A., 1990, MNRAS 244, 130
Harris A.I., Hills R.E., Stutzki J., Graf U.U., Russell A.P.G., Genzel R., 1991, ApJL 382, L75
Henkel C., Whiteoak J.B., Nyman L.-A., Harju J., 1990, A&A 230, L5
Henkel C., Baan W.A., Mauersberger R., 1991, A&AR 3, 47
Herbst E., Leung C.M., 1989, ApJS 69, 271
IRAS 1989, Catalogued Galaxies and Qyasars in the IRAS Survey, Version 2, produced by L. Fullmer & C. Lonsdale, NASA-JPL D-1932 (Pasadena)
Irvine W.M., Goldsmith P.F., Hjalmarson A., 1987, in: Hollenbach D.J., Thronson H.A. (eds.) Interstellar Processes, Reidel, Dordrecht, p. 561
Israel F.P., van Dishoeck E.F., Baas F., Koornneef J., Black J.H., de Graauw T., 1990, A&A 227, 342
Israel F.P., van Dishoeck E.F., Baas F., de Graauw T., Phillips T.G., 1991, A&A 245, L13
Mauersberger R., Henkel C., 1989, A&A 223, 79
Mauersberger R., Henkel C., Sage L.J., 1990, A&A 236, 63
Nguyen-Q-Rieu, Nakai N., Jackson J.M., 1989, A&A 220, 57
Nguyen-Q-Rieu, Jackson J., Henkel C., Mauersberger R., 1991, in: Combes F., Casoli F. (eds.) Dynamics of Galaxies and Their Molecular Cloud Distributions, Kluwer, Dordrecht, p. 299
Quillen A.C., de Zeeuw P.T., Phinney E.S., Phillips T.G., 1992, ApJ 391, 121

Rice W., Lonsdale C.J., Soifer B.T., Neugebauer G., Kopan E.L., Lloyd L.A., de Jong T., Habing H.J., 1988, ApJS 68, 91
Rowan-Robinson M., Crawford J., 1989, MNRAS 238, 523
Sargent A.I., Sanders D.B., Phillips T.G., 1989, ApJ 346, L9
Solomon P.M., Downes D., Radford S.J.E., 1992, ApJL (submitted)
Toomre A., 1977, in: The Evolution of Galaxies and Stellar Populations (Yale Univ. Obs.: New Haven), p. 401
Turner B.E., 1985, ApJ 299, 312
Wall W.F., 1991, Ph.D. Thesis University of Texas at Austin (USA)
Wall W.F., Jaffe D.T., Israel F.P., Bash F.N., 1991, ApJ 380, 384
Whiteoak J.B., 1986, Proc. Astron. Soc. Aust. 6, 467
Whiteoak J.B., Bunton J.D., 1985, Proc. Astron. Soc. Aust. 6, 171
Whiteoak J.B., Gardner F.F. 1986, MNRAS 222, 513
Whiteoak J.B., Wilson W.E., 1990, MNRAS 245, 665
Whiteoak J.B., Dahlem M., Wielebinski R., Harnett J.L., 1990, A&A 231, 25